Supporting Information

Enhanced visualization of cell surface glycans via hybridization chain reaction

Xiaohong Wen,‡ Baoyin Yuan,‡ Junxun Zhang, Xiangxian Meng, Qiuping Guo,* Lie Li, Zenghui Li, Huishan Jiang and Kemin Wang*

State Key Laboratory of Chemo/Biosensing and Chemometrics, College of Chemistry and Chemical Engineering, Key Laboratory for Bio-Nanotechnology and Molecular Engineering of Hunan Province, Hunan University, Changsha 410082, China.

To whom correspondence should be addressed:

*Email: guoqping@126.com; kmwang@hnu.edu.cn.

Tel/Fax: +86-731-88821566.

Experimental Section

Chemicals and materials. N-Azidoacetylgalactosamine-tetraacylated (Ac$_4$GalNAZ), N-azidoacety-lmannosamine-tetraacylated (Ac$_4$ManNAZ), and trypsin were purchased from Thermo Scientific (USA). SYBR Gold nucleic acid dye were purchased from Invitrogen (USA). Roswell Park Memorial Institute 1640 (RPMI-1640) and fetal bovine serum (FBS) were provided by Hyclone (USA). DNA sequences used in the experiment were synthesized by Sangon Biotechnology Co., Ltd. (Shanghai, China). All DNA sequences used in this work are listed in Table S1. The water used throughout this work was produced by the Milli-Q water purification system (Millipore SystemInc., USA). Dulbecco's phosphate-buffered saline (D-PBS) was purchased from Gibco (USA). Tunicamycin was purchased from Solarbio (Beijing, China). Other chemicals were of analytical grade at least.

Cell lines and cell culture. Hepatocellular carcinoma SMMC-7721 cells used in the experiment were obtained from the cell bank of the Committee on Type Culture Collection of the Chinese Academy of Sciences (Shanghai, China). Cervical cancer cell line HeLa, CEM, Tca8113 and HepG2 was purchased from American Type Culture Collection. All cells were cultured in basic RPMI 1640 medium supplemented with 12% fetal bovine serum (FBS) and 0.02% penicillin−gentamicin (200 μg/mL) at 37 °C in a humidified incubator containing 5% CO$_2$ by volume. Both cell subculture and pretreatment were conducted at a clean bench.

Preparation of the HCR-based heteroduplexes. The probe H1, H2, and DBCO-labeled trigger were dissolved in D-PBS supplemented with 5 mM Mg^{2+}, respectively. Then the probe H1 (20 μM), H2 (20 μM) and DBCO-labeled trigger (10 μM) were mixed together according to the system in the table S1, then heated at 95 °C for 5 min and cooled at 37 °C for 90 min for the formation of the heteroduplexes.

Agarose gel electrophoresis. The obtained heteroduplexes were characterized by 2.5% agarose gel electrophoresis (100 V, 45 min), and after being stained with SYBR Gold,

the gel was imaged by a C600 multifunctional molecular imaging system (Azure Biosystems, USA). For UV imaging, the gel was excited using 302-nm light and collected with a 595/55-nm filter; for TR fluorescent imaging, the gel was excited using 628-nm light and collected with a 676/28-nm filter.

Metabolic glycan labeling. SMMC-7721 cells, HeLa cells, CEM cells, Tca8113 cells and HepG2 cells were seeded at a density of 2000 cells in 100 μL of media on glass-bottom dishes (In Vitro Scientific, USA) and cultured in 1640 medium containing 5 μM $Ac_4GalNAz$ or $Ac_4ManNAz$ for 48 h, respectively. After being washed with D-PBS three times, the cells were used for subsequent experiments.

Flow cytometry assays. To test the effect of click chemistry on cells and nanoassemblies, the SMMC-7721 cells were incubated with 50 nM TR-labeled random sequence or nanoassemblies in 200 μL of binding buffer at 4 °C for 90 min. After being washed with binding buffer twice, the cells were analyzed with a flow cytometer (Gallios, Beckman Coulter, USA) by counting 10 000 events. The TR fluorescence signal was collected in FL3 with a 543-nm laser and a 560-nm long-pass filter.

In order to improve the imaging contrast of glycoprotein with TR-labeled nanoassemblies, the probe concentration, incubation temperature and incubation time were optimized, respectively. When the concentration was optimized, the cells were incubated with 5, 10, 25, 50, 100, 200 nM TR-labeled nanoassemblies in 200 μL binding buffer at 4 °C for 90 min, respectively. After being washed with binding buffer twice, the cells were analyzed with a flow cytometer by counting 10 000 events. When the incubation temperature was optimized, the cells were incubated with 50 nM TR-labeled nanoassemblies in 200 μL binding buffer at 4, 25, 37, 40 °C for 90 min, respectively. After being washed with binding buffer twice, the cells were analyzed with a flow cytometer by counting 10 000 events. Similarly, when the incubation time was optimized, the cells were incubated with 50 nM TR-labeled nanoassemblies in 200 μL binding buffer at 4 °C for 30, 60, 90, 120, 150 min, respectively. After being

washed with binding buffer twice, the cells were analyzed with a flow cytometer by counting 10 000 events.

To visualize the glycosylation states under drug treatment by the HCR strategy, the HepG2 cells were pretreated with the mixture of $Ac_4ManNAz$ and TM of different doses (0, 25, 50, 100, and 150 ng/ml) for 48 h to inhibit N-glycosylation in living cells, respectively. Then, the treated cells were incubated with 50 nM nanoassemblies in 200 µL of binding buffer at 4 °C for 90 min. After being washed with binding buffer twice, the cells were analyzed with a flow cytometer (Gallios, Beckman Coulter, USA) by counting 10 000 events. The TR fluorescence signal was collected in FL6 with a 543-nm laser and a 560-nmlong-pass filter.

Fluorescence intensity detection. For the fluorescence intensity detection, the cells were cultured in a 6-well Assay Black Plate (Corning). The HCR reaction was performed as described above. After the above assembly process, the DBCO-nanoassemblies can be crosslinked with cell surface glycoproteins by the click chemical reaction. Next, the slide was washed with D-PBS twice, fluorescence intensity data were collected in triplicate by a microplate reader.

Cytotoxicity assay in vitro. Cells were seeded onto 96-well plates at the density of $1×10^4$ cells per well, the cells were cultured in RPMI 1640 medium which containing 10% FBS and 5 µM Ac4ManNAz, incubated under a humidified atmosphere of 5% CO2+95% air overnight. Then removing RPMI 1640 medium, the cells were treated with TR-labeled nanoassemblies for 45 min. After washing with WB twice, the cells were recultured for 48 h. For the control, the medium was added instead of TR-labeled nanoassemblies. Subsequently removing all of supernatants in 96-well plate, the cells were further incubated with 20 µL MTT (0.5 mg•mL-1) and 180 µL medium for 4 h. Thereafter, the medium was carefully removed and added DMSO (150 µL) into each well. At once the 96-well plate was shook for 10 min. Finally, the optical density (OD) was measured at 490 nm on a multi-detection microplate reader (M1000 Pro, TECAN). Survival rate of cells was calculated as follows:

The cell viability (%) = (OD$_{treated}$ / OD$_{control}$) × 100%.

Confocal Imaging. For HCR-based enhanced imaging of cell-surface glycosylation, the SMMC-7721 cells and HeLa cells that were subjected to metabolic glycan labeling were incubated with the TR-labeled nanoassemblies at 4 °C for 90 min, followed by washing with D-PBS three times, and imaged with a FV500 (Olympus, Japan) laser scanning confocal microscope (LSCM). TR fluorescence was excited at 543 nm and collected with a 560-nm long-pass filter.

Supporting Tables:
Table S1. List of DNA sequences.

| name	sequence(5′→3′)
Trigger	5'-AGT TGT AGT CAG ACT ATT CGA T TTT TTT TTT TTT TTT-DBCO-3'
unvarnished Trigger	5'-AGT TGT AGT CAG ACT ATT CGA T TTT TTT TTT TTT TTT-3'
H1	5'-ATC GAA TAG TCT GAC TAC AAC TTG AAA CAG TTG TAG TCA GAC TA-TR-3'
H2	5'-TR-AGT TGT AGT CAG ACT ATT CGA TTA GTC TGA CTA CAA CTG TTT CA-3'

Supporting Figures:
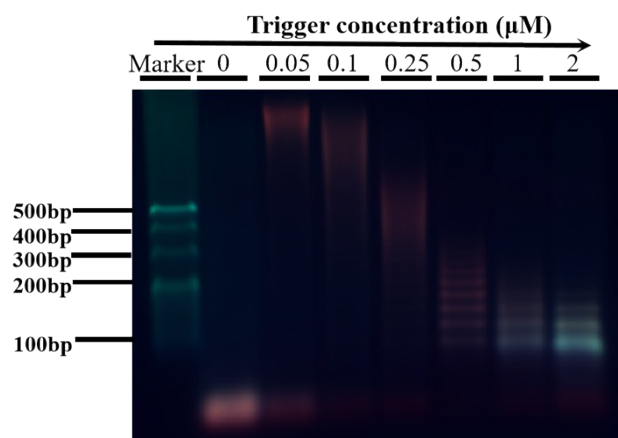
Figure S1. Fluorescent imaging of optimization of the ZYsls-trigger concentration for HCR amplification. Optimization of the trigger concentration for formation of nanoassemblies by agarose gel electrophoresis. Increasing concentrations of trigger, 0, 1:100, 1:50, 1:20, 1:10, 1:5, 1:2.5, were added to mixtures of H1 and H2 (5 μM each), followed by fluorescent imaging of agarose gel electrophoresis. The results demonstrated that a 1:50 ratio was the best, which was used in subsequent experiments. The marker used is 20 bp DNA Ladder.
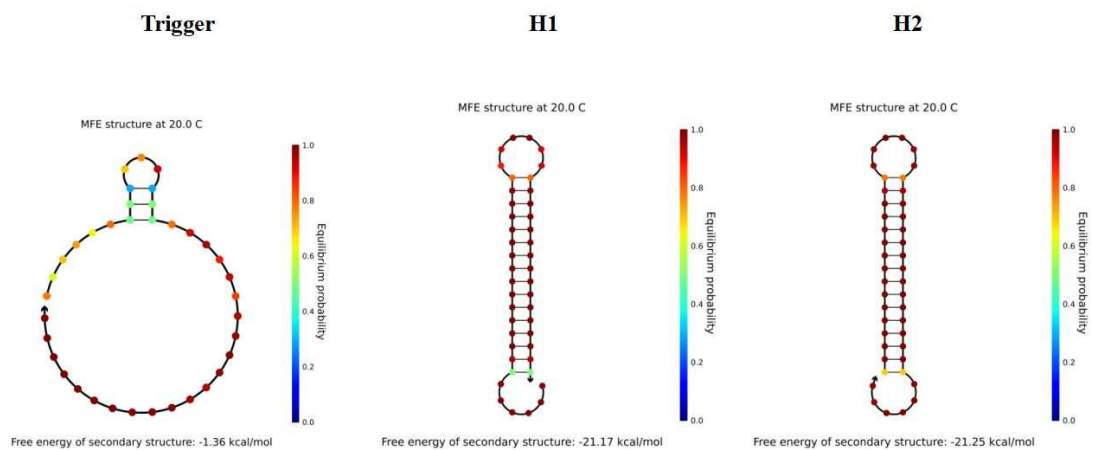
Trigger **H1** **H2**

Figure S2. Simulation of trigger, H1 and H2 secondary structure in HCR reaction by Mfold software.
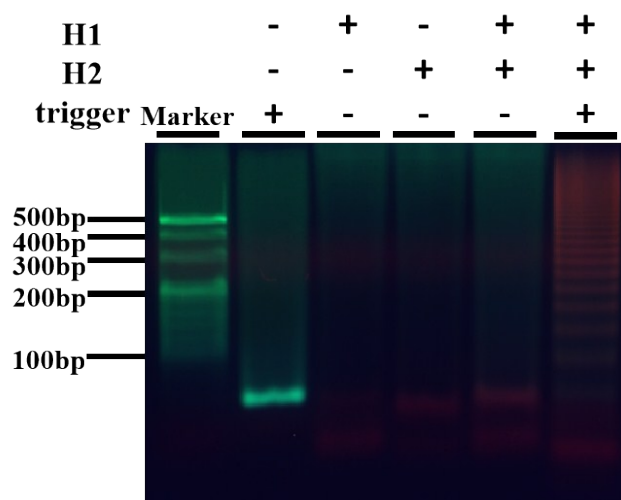
Figure S3. Fluorescent imaging of the HCR polymerization initiated by trigger. Agarose gel electrophoresis followed by TR fluorescent imaging demonstrating the polymerization of nanoassemblies initiated by trigger. H1, H2 and trigger were labeled with TR fluorescent groups, respectively. The marker used is 20 bp DNA Ladder.
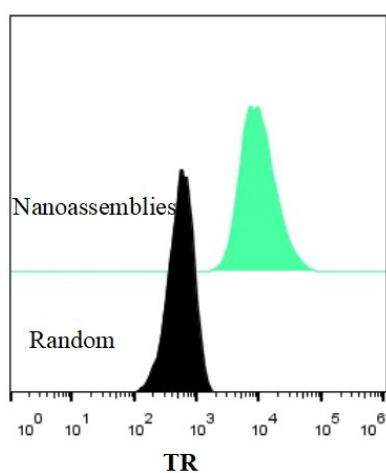
Figure S4. Flow cytometric assays of crosslinking abilities of DBCO-nanoassemblies to SMMC-7721 cells. Flow cytometric assays of crosslinking abilities of TR-labeled random sequence, and TR-labeled DBCO-nanoassemblies to target 7721 cells. Samples were washed three times with binding buffer before flow cytometric assays. Flow cytometry histograms showing that TR-labeled nanoassemblies could be displayed on the cell surface. The TR fluorescence signal was collected in FL6 with a 633-nm laser and a 660-nm long-pass filter.
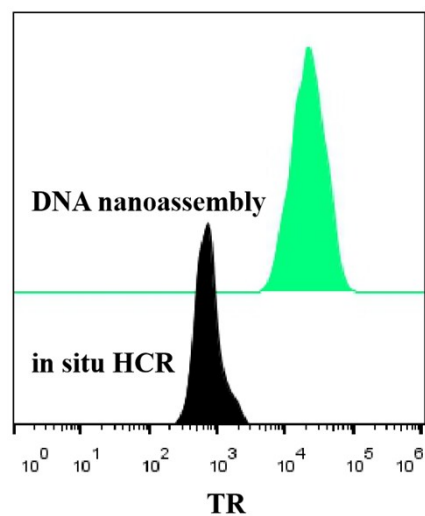
Figure S5. Comparision of in situ HCR with the present method by flow cytometry analysis. Flow cytometry histograms showing that our method can achieve better amplification effect at the same probe concentration. The TR fluorescence signal was collected in FL3 with a 543-nm laser and a 560-nm long-pass filter.
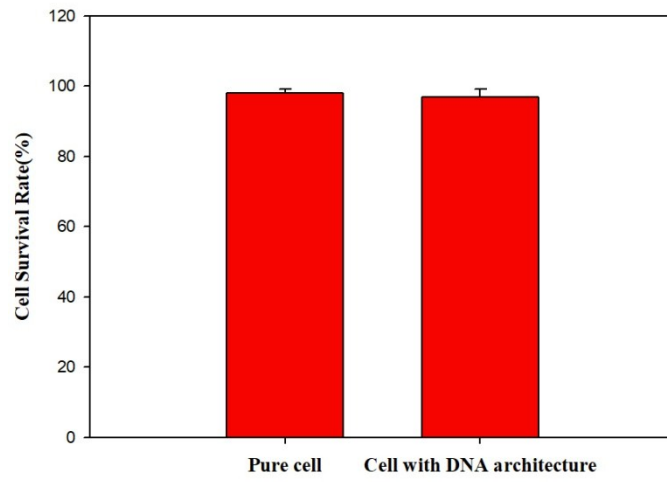
Figure S6. Quantitative detection of cells viability following incubating with or without DNA architecture and next reculture for 48 h. The date are shown as mean ± SD (n = 3).
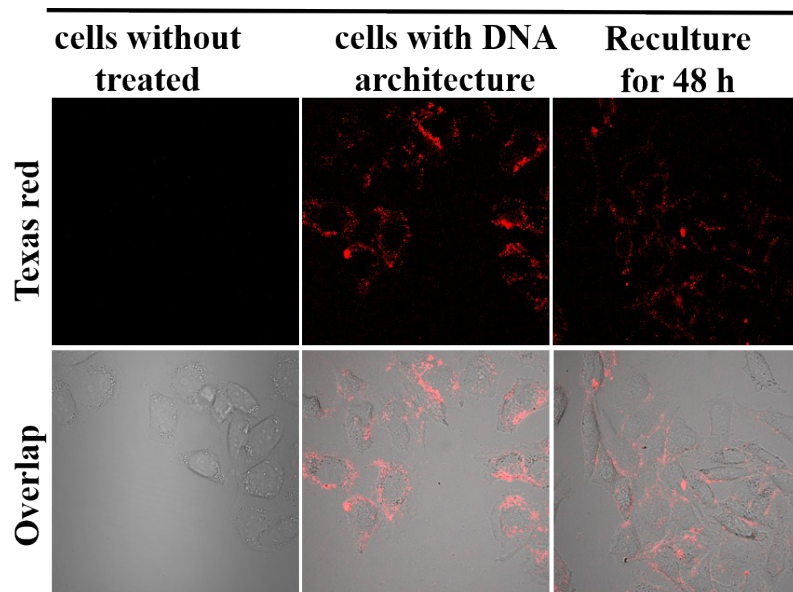
Figure S7. Confocal imaging of cell morphology after HepG2 cells incubated with DNA architecture for 48 h. Cells without any treated (left) and cells with DNA architecture (middle) were imaged by confocal imaging. Then, confocal imaging of cells with DNA architecture after re-cultured for 48 h (right). It is noteworthy that the TR fluorescence was slightly quenched during the re-culture process. The upper are fluorescence images, the lower are the overlays of the fluorescence channel and the bright-field channel. TR fluorescence was excited using a 543-nm laser and collected with a 560-nm long-pass filter. The fluorescence signal was collected by a 100× objective.
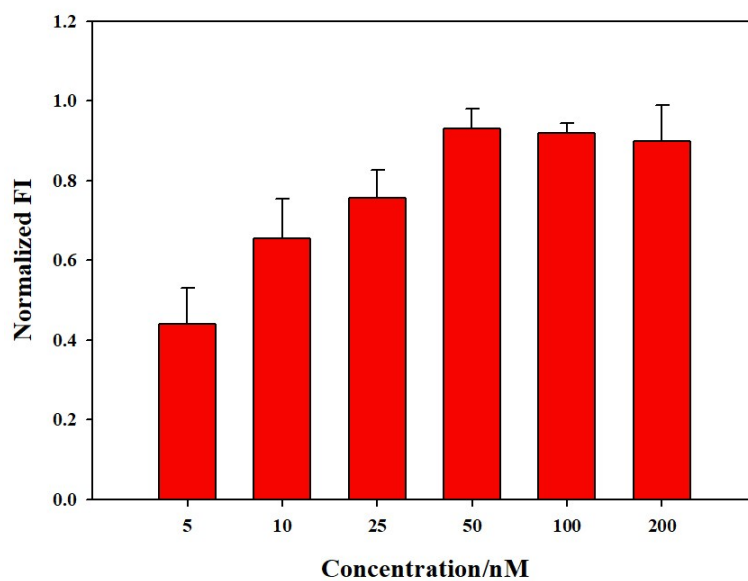
Figure S8. Optimization of probe concentration of the nanoassemblies to SMMC-7721 cells by flow cytometry. Error bars indicate the standard deviations of three experiments. The TR fluorescence signal was taken from geometric mean and collected in FL3 with a 543-nm laser and a 560-nm long-pass filter. The data represent means ± SD (n = 3).
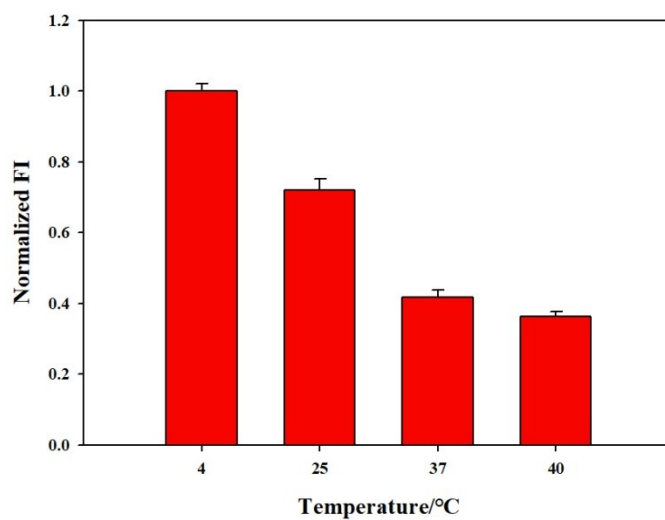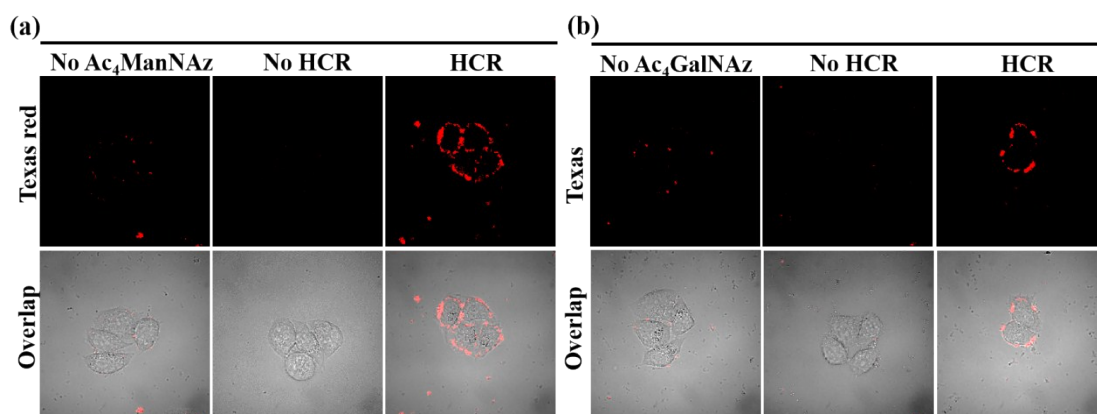
Figure S9. Flow cytometric assays of incubation temperature of the nanoassemblies to SMMC-7721 cells. Error bars indicate the standard deviations of three experiments. The TR fluorescence signal was taken from geometric mean and collected in FL3 with a 543-nm laser and a 560-nm long-pass filter. The data represent means ± SD (n = 3).
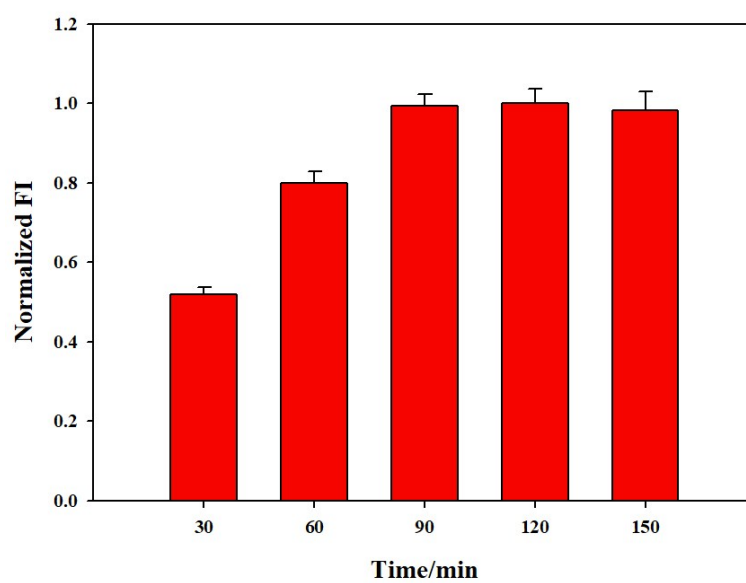
Figure S10. Optimization of incubation time of 7721 cells to nanoassemblies by flow cytometry. The TR fluorescence reached the highest when the time was 90 min. The data represent means ± SD (n = 3).

(a)

	No Ac$_4$ManNAz	No HCR	HCR
Texas red			
Overlap			

(b)

	No Ac$_4$GalNAz	No HCR	HCR
Texas			
Overlap			

Figure S11. Fluorescence detection of HeLa cells treated with Ac$_4$ManNAz (a) or Ac$_4$GalNAz (b). A comparison of fluorescence images upon treatment with 5.0 µM different unnatural monosaccharides. The upper are fluorescence images, the lower are the overlays of the fluorescence channel and the bright-field channel. TR fluorescence was excited using a 543-nm laser and collected with a 560-nm long-pass filter. The fluorescence signal was collected by a 100× objective.
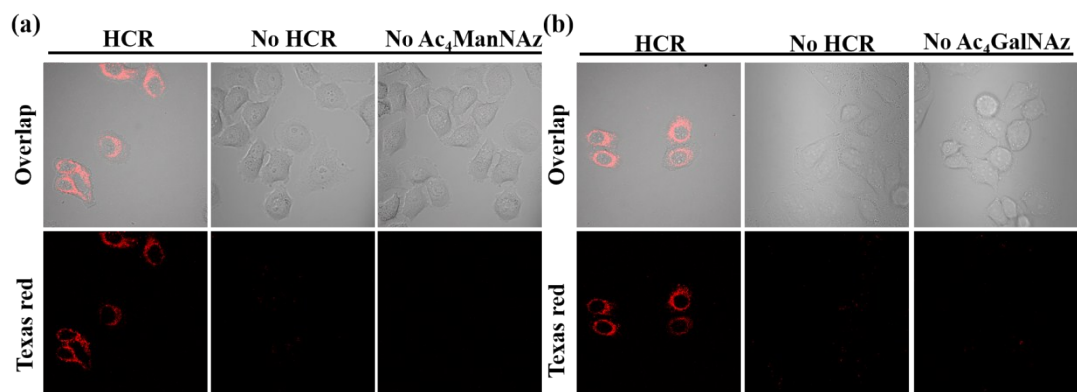
Figure S12. Fluorescence detection of Tca8113 cells treated with Ac$_4$ManNAz (a) or Ac$_4$GalNAz (b). A comparison of fluorescence images upon treatment with 5.0 μM different unnatural monosaccharides. The lower are fluorescence images, the upper are the overlays of the fluorescence channel and the bright-field channel. TR fluorescence was excited using a 543-nm laser and collected with a 560-nm long-pass filter. The fluorescence signal was collected by a 100× objective.

(a)

	HCR	No HCR	No Ac₄ManNAz
Overlap			
Texas red			

(b)

	HCR	No HCR	No Ac₄GalNAz
Overlap			
Texas red			
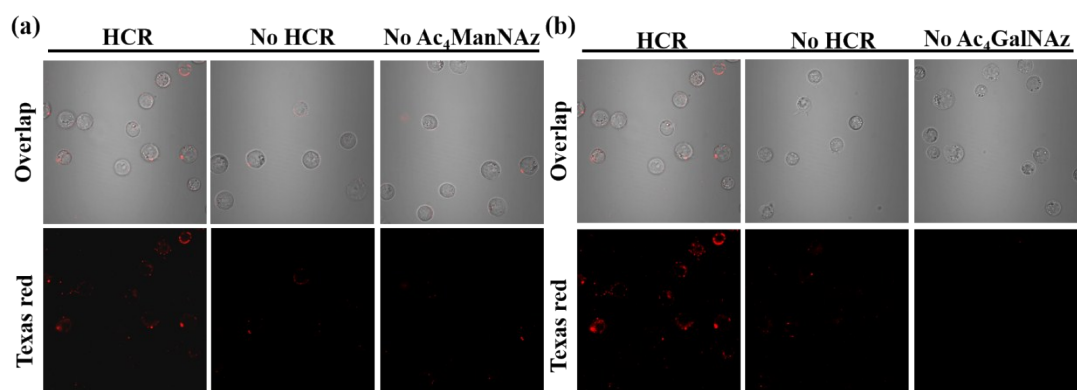
Figure S13. Fluorescence detection of CEM cells treated with Ac$_4$ManNAz (a) or Ac$_4$GalNAz (b). A comparison of fluorescence images upon treatment with 5.0 μM different unnatural monosaccharides. The lower are fluorescence images, the upper are the overlays of the fluorescence channel and the bright-field channel. TR fluorescence was excited using a 543-nm laser and collected with a 560-nm long-pass filter. The fluorescence signal was collected by a 100× objective.
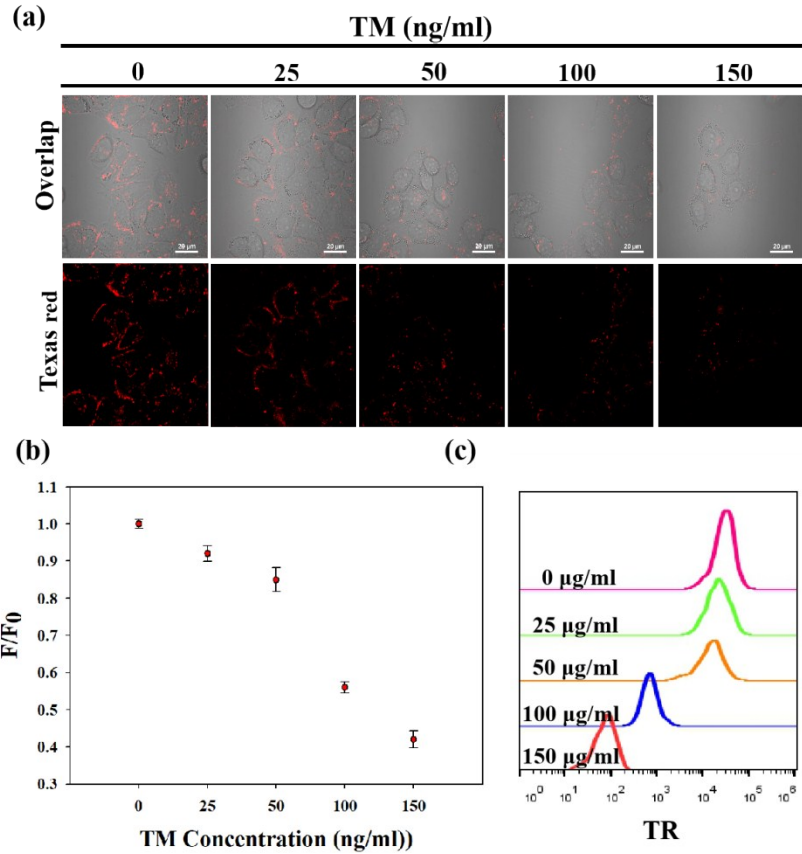
Figure S14. (a) Confocal imaging of HepG2 cells pretreated with a mixture of 5 μM Ac$_4$ManNAz and TM at different concentrations (0, 25, 50, 100, and 150 ng/ml) with HCR amplification. Scale bar: 20 μm. (b) Quantitative confocal imaging intensity and (c) flow cytometry assay of HCR fluorescence. TR fluorescence was excited using a 543-nm laser and collected with a 560-nm long-pass filter.